Journal of Organometallic Chemistry 745-746 (2013) 64–70

Contents lists available at ScienceDirect

Journal of Organometallic Chemistry

journal homepage: www.elsevier.com/locate/jorganchem

Synthesis, X-ray structure, electrochemical properties and cytotoxic effects of new arene ruthenium(II) complexes

Adam Pastuszko [a], Karolina Niewinna [b], Malgorzata Czyz [b], Andrzej Jóźwiak [c], Magdalena Małecka [d], Elzbieta Budzisz [a,*]

[a] Department of Cosmetic Raw Materials Chemistry, Faculty of Pharmacy, Medical University of Łódź, Muszynski 1 Street, 90-151 Łódź, Poland
[b] Department of Molecular Biology of Cancer, Medical University of Łódź, Mazowiecka 6/8 Street, 92-215 Łódź, Poland
[c] Department of Organic Chemistry, Faculty of Chemistry, University of Łódź, Tamka 12, 91-403 Łódź, Poland
[d] Department of Structural Chemistry and Crystallography, University of Łódź, Pomorska 163/165, 90-236 Łódź, Poland

ARTICLE INFO

Article history:
Received 27 May 2013
Received in revised form
4 July 2013
Accepted 5 July 2013

Keywords:
Synthesis
Arene ruthenium(II) complexes
X-ray structure
Cytotoxic effect
Cyclic voltammetry

ABSTRACT

A series of novel half-sandwich organoruthenium(II) complexes with the general formula [(η^6-arene)Ru(L)Cl_2] (where L = flavone, chromone or benzofuranone derivatives) have been synthesized. All the ligands in the reaction with [(η^6-*p*-cymene)RuCl)$_2$(μ-Cl)$_2$] form monodentate compounds, which were fully characterized by elemental analysis, MS, UV–Vis, IR and NMR spectroscopy. The molecular structure of one of the complexes [(η^6-*p*-cymene)Ru(7-amino-3*H*-benzofuran-1-one-κ^1-N)Cl_2] was determined by X-ray crystallography. The redox properties of the complexes were monitored by cyclic voltammetry. The cytotoxicity of all obtained compounds has also been evaluated on several melanoma and leukemic cell lines.

1. Introduction

Organometallic ruthenium(II) complexes have attracted considerable interest as potential anticancer agents because of their low toxicity, often good aqueous solubility [1] and their efficacy against platinum drug resistant tumors [2–4]. Ruthenium(II) and ruthenium(III) complexes have similar ligand-exchange kinetics to those of platinum complexes. Ruthenium(II) complexes bearing a π-bonded arene ligand and other mono- or bidentate ligands are considered to be promising candidates for anticancer treatment [5]. The arene substituent is known to stabilize ruthenium in its +2 oxidation state and the arene ligand is relatively inert toward displacement under physiological conditions [6]. All substituents, the monodentate ligand and the bidentate ligand as well the arene substituent possess influent on the pharmacological properties of arene–Ru(II) complexes [7]. Substitution of chloride by other halides, such as iodide has only a small effect on the cytotoxicity of complexes with ethylenediamine as ligand [8]. The size of the coordinated arene substituent appears to increase on activity. More hydrophobic arene ligand and bidentate chelating ligand cause the higher cytotoxicity. Moreover, complexes which lack of NH groups on the coordinated ligand are often inactive [9]. In addition, the redox potential between the different accessible oxidation states occupied by ruthenium complexes enables to catalyze oxidation and reduction reactions, depending on physiological environment.

On the other hand the ligands selected for the current experiments belong to the well known group of the compounds in plants – flavonoids. These derivatives are naturally occurring compounds which are able to induce cytotoxic effect in various cell lines. Due to their miscellaneous activities, such as anticancer [10], antioxidant, antiproliferative [11], anti-HIV, anti-inflammatory [12], and many other activities, they are used in several areas like chemistry, biochemistry, genetics, cellular and molecular biology. Moreover, flavonoids form metal ions complexes with important biological activity [13]. Copper(II) complexes show higher anti-inflammatory activity than free flavonoids [14]. From the above results the approach to attach a bioactive ligand to arene ruthenium(II) moiety is very promising and important in investigating of biological properties.

In this paper, we report the synthesis and characterization of (η^6-*p*-cymene)Ru(II) complexes with aminochromone derivatives and its analogs. The cytotoxic effect has been assayed on human melanoma A375, DMBC11, DMBC12 and leukemic K562 cell lines.

* Corresponding author. Tel.: +48 42 272 55 95; fax: +48 42 678 83 98.
E-mail address: elzbieta.budzisz@umed.lodz.pl (E. Budzisz).

0022-328X/$ – see front matter © 2013 Elsevier B.V. All rights reserved.
http://dx.doi.org/10.1016/j.jorganchem.2013.07.020

2. Experimental

2.1. Material and methods

All substances were used without further purification. The *p*-cymeneruthenium(II) dichloride, 3-nitrophthalic anhydride, 7-amino-2-methylochromone, 7-aminoflavone and 6-aminoflavone were purchased from Aldrich. Solvents for synthesis (dichoromethane, isopropanol, acetone, diethyl ether) were reagent grade or better. The melting points were determined using an Electrothermal 1A9100 apparatus and they are uncorrected. The IR spectra were recorded on an FTIR–8400S Shimadzu Spectrophotometer in KBr. The ^{1}H NMR spectra were registered at 300 MHz on a Varian Mercury spectrometer. The MS–FAB were measured on Finnigan Matt 95 mass spectrometer. Elemental analyses were performed by using a Perkin Elmer PE 2400 CHNS analyzer. The ligands **1**–**3** were commercially available. Ligands **4** and **5** were prepared according to published methods.

2.1.1. Synthesis of [(η^6-p-cymene)Ru(6-amino-2-phenyl-4H-benzo pyran-4-one-κ^1-N)Cl_2] (**1a**)

To a stirred solution of 6-aminoflavone (94.89 mg, 0.4 mmol) in isopropanol (8 ml) and dichloromethane (4 ml) a solution of ruthenium *p*-cymene (122.48 mg, 0.2 mmol) in dichloromethane (4 ml) was added dropwise. The reaction mixture was stirred at room temperature for 24 h. The resulting precipitate was separated and dried under reduced pressure. Yield: 152.5 mg (70%). M.p.: 235–238 °C. Anal. Calc. for $C_{25}H_{25}NO_2RuCl_2$ (543.433 g/mol): C, 55.25; H, 4.63; N, 2.58. Found: C, 55.20; H, 4.14, N, 2.75. IR (KBr, cm^{-1}) (selected bands): ν(C–NH_2) 3228, 3191; ν(C=O) 1619. ^{1}H NMR (300 MHz, $CDCl_3$) δ (ppm): 1.28 (d, 6H, $^3J_{HH}$ = 7.0 Hz), 2.18 (s, 3H), 2.93 (m, 1H), 4.91 (s, 2H), 4.98 (d, 2H, $^3J_{HH}$ = 5.9 Hz), 5.09 (d, 2H, $^3J_{HH}$ = 5.9 Hz), 5.38 (d, 2H, $^3J_{HH}$ = 5.9 Hz), 5.50 (d, 2H, $^3J_{HH}$ = 5.9 Hz), 6.90 (s, 1H), 8.05–7.56 (m, 8H). MS–FAB (*m*/*z*): 543 ($LRuCl_2$), 508 ($LRuCl^+$), 472 (LRu^{2+}), 238 (L).

2.1.2. Synthesis of [(η^6-p-cymene)Ru(7-amino-2-phenyl-4H-benzo pyran-4-one-κ^1-N)Cl_2] (**2a**)

To a stirred solution of 7-aminoflavone (118.63 mg, 0.5 mmol) in dichloromethane (8 ml) a solution of ruthenium *p*-cymene (153.09 mg, 0.25 mmol) in dichloromethane (5 ml) was added dropwise. The reaction mixture was stirred at room temperature for 24 h. The resulting precipitate was separated and dried under reduced pressure. Yield: 204.7 mg (71%). M.p.: 207–209 °C. Anal. Calc. for $C_{25}H_{25}NO_2RuCl_2$ (543.433 g/mol): C, 51.82; H, 5.04; N, 2.41. Found: C, 51.99; H, 4.46; N, 2.36. IR (KBr, cm^{-1}) (selected bands): ν(C–NH_2) 3345, 3213; ν(C=O) 1647. ^{1}H NMR (300 MHz, $CDCl_3$) δ (ppm): 1.28 (d, 6H, $^3J_{HH}$ = 6.8 Hz), 2.17 (s, 3H), 2.93 (m, 1H), 4.98 (d, 2H, $^3J_{HH}$ = 5.8 Hz), 5.12 (d, 2H, $^3J_{HH}$ = 5.8 Hz), 5.35 (d, 2H, $^3J_{HH}$ = 6.0 Hz), 5.48 (d, 2H, $^3J_{HH}$ = 5.9 Hz), 6.78 (s, 1H), 8.13–7.54 (m, 8H). MS–FAB (*m*/*z*): 544 ($LRuCl_2$ + 1H), 508 ($LRuCl^+$), 475 (LRu^{2+}), 238 (L).

2.1.3. Synthesis of [(η^6-p-cymene)Ru(7-amino-2-methyl-4H-benzo pyran-4-one-κ^1-N)Cl_2] (**3a**)

To a stirred solution of 7-amino-2-methylochromone (87.60 mg, 0.5 mmol) in dichloromethane (8 ml) a solution of ruthenium *p*-cymene (153.10 mg, 0.25 mmol) in dichloromethane (5 ml) was added dropwise. The reaction mixture was stirred at room temperature for 24 h. The resulting precipitate was separated and dried under reduced pressure. Yield: 129.0 mg (51%). M.p.: 211–213 °C. Anal. Calc. for $C_{20}H_{23}NO_2RuCl_2$ (481.385 g/mol): C, 47.25; H, 5.15; N, 2.75. Found: C, 47.23; H, 4.71; N, 2.73. IR (KBr, cm^{-1}) (selected bands): ν(C–NH_2) 3202, 3101; ν(C=O) 1618. ^{1}H NMR (300 MHz, $CDCl_3$) δ (ppm): 1.27 (d, 6H, $^3J_{HH}$ = 7.0 Hz), 2.16 (s, 3H), 2.37 (s, 3H), 2.93 (m, 1H), 4.97 (d, 2H, $^3J_{HH}$ = 5.9 Hz), 5.09 (d, 2H, $^3J_{HH}$ = 6.2 Hz), 5.35 (d, 2H, $^3J_{HH}$ = 6.2 Hz), 5.48 (d, 2H, $^3J_{HH}$ = 5.9 Hz), 8.10–6.92 (m, 3H), 6,13 (s, 1H). MS–FAB (*m*/*z*): 481 ($LRuCl_2$), 446 ($LRuCl^+$), 410 (LRu^{2+}), 176 (L).

2.1.4. Synthesis of [(η^6-p-cymene)Ru(5-amino-8-methyl-4H-1-benzopyran-4-one-κ^1-N)Cl_2] (**4a**)

To a stirred solution of 5-amino-8-methyl-4*H*-benzopyran-4-one (72.89 mg, 0.416 mmol) in dichloromethane (5 ml) a solution of ruthenium *p*-cymene (124.20 mg, 0.208 mmol) in dichloromethane (5 ml) was added dropwise. The reaction mixture was stirred at room temperature for 24 h. The resulting precipitate was separated and dried under reduced pressure. Yield: 108.1 mg (54%). M.p.: 190–191 °C. Anal. Calc. for $C_{20}H_{23}NO_2RuCl_2$ (481.385 g/mol): C, 49.89; H, 4.82; N, 2.91. Found: C, 49.34; H, 4.77; N, 2.84. IR (KBr, cm^{-1}) (selected bands): ν(C–NH_2) 3544, 3477; ν(C=O) 1640. ^{1}H NMR (300 MHz, $CDCl_3$) δ (ppm): 1.28 (d, 6H, $^3J_{HH}$ = 6.9 Hz), 2.10 (s, 3H), 2.18 (s, 3H), 2.94 (m, 1H), 5.00 (d, 2H, $^3J_{HH}$ = 5.9 Hz), 5.05 (d, 2H, $^3J_{HH}$ = 5.9 Hz), 5.36 (d, 2H, $^3J_{HH}$ = 5.9 Hz), 5.49 (d, 2H, $^3J_{HH}$ = 5.9 Hz), 7.98–6.27 (m, 4H). MS–FAB (*m*/*z*): 446 ($LRuCl^+$), 410 (LRu^{2+}), 176 (L).

2.1.5. Synthesis of [(η^6-p-cymene)Ru(7-amino-3H-benzofuran-1-one-κ^1-N)Cl_2] (**5a**)

To a solution of 7-aminophtalide (59.65 mg, 0.4 mmol) in dichloromethane (5 ml) a solution of ruthenium *p*-cymene (122.48 mg, 0.2 mmol) in dichloromethane (5 ml) was added dropwise. The reaction mixture was stirred at room temperature for 24 h. The resulting precipitate was separated and dried under reduced pressure. Yield: 104.9 mg (59%). M.p.: 221–223 °C. Anal. Calc. for $C_{18}H_{21}NO_2RuCl_2$ (455.347 g/mol): C, 47.48; H, 4.65; N, 3.08. Found: C, 47.15; H, 4.75, N, 2.97. IR (KBr, cm^{-1}) (selected bands): ν(C–NH_2) 3264, 3181; ν(C=O) 1741. ^{1}H NMR (300 MHz, $CDCl_3$) δ (ppm): 1.29 (d, 6H), 2.18 (s, 3H), 2.94 (m, 1H), 5.26 (s, 4H), 5.36 (d, 2H, $^3J_{HH}$ = 5.9 Hz), 5.49 (d, 2H, $^3J_{HH}$ = 5.9 Hz), 7.62–7.21 (m, 3H). MS–FAB (*m*/*z*): 460 ($LRuCl_2$), 154 (L).

2.2. Crystallographic analysis

Very small crystals were obtained by recrystallization from dichloromethane/hexane by diffusion technique. An orange shaped crystal of dimension 0.05 × 0.04 × 0.01 mm was used to collect data in 100 K. 11,469 reflections were measured with omega scan mode on SuperNova diffractometer using MoKα radiation (λ = 0.7107 Å). The structure was solved by direct methods with the program SHELXS-97 and refined by full-matrix least-squares method on F^2 with SHELXL-97 [15]. The non-H atoms were refined anisotropically. All hydrogen position were placed geometrically and refined using a riding model, with $U_{iso}(H) = x\ U_{eq}(C)$ where x = 1.5 for methyl groups and 1.2 for all others. C–H distances were fixed for methyl group at 0.96 Å, for aromatic at 0.93 Å, for methine 0.98 Å, for methylene 0.97 Å and for NH_2 group 0.9 Å. Final results are: $R1$ = 3.47% and 3.04% for all and observed reflections, respectively. The largest difference peak and hole are: 0.52 and −0.56 e/Å^3. Atomic coordinates and relevant data have been deposited at the Cambridge Crystallographic Data Centre as supplementary publication number CCDC 936546. These data can be obtained free of charge from CCDC *via* http://www.ccdc.cam.ac.uk/products/csd/request/.

2.3. Biological evaluation

Three melanoma cell lines were used in the current study. Leukemia represented by K562 cell line was maintained in RPMI1640 medium supplemented with 10% FBS and antibiotics.

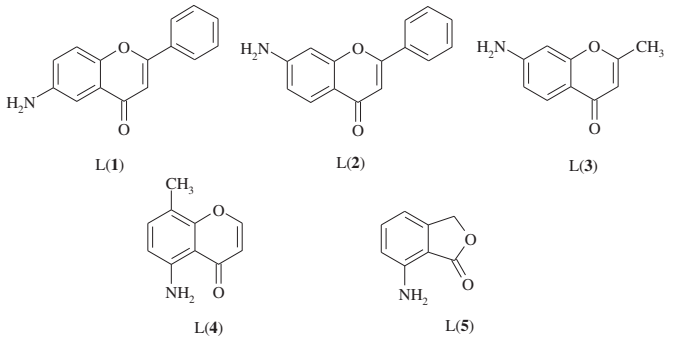

Fig. 1. Selected ligands **1**–**5**.

A375 human melanoma cell line with high metastatic potential (a gift from Prof. Piotr Leidler, Jagiellonian University, Poland) was also maintained in RPMI1640 medium supplemented with 10% FBS and antibiotics. DMBC11 and DMBC12 cell lines, derived from patients with nodular melanoma (NM), were established and maintained in our laboratory as described before [16].

2.3.1. Measurement of cell number

Cancer cells were counted after staining with Trypan blue (Sigma–Aldrich) and plated at a density of 2–4 $\times$ 10^3 viable cells per well in 96-well plates. Cells were cultured for 2 days with tested compounds at indicated concentrations. An acid phosphatase activity (APA) assay was used to measure viable cell number in the culture. Briefly, the plates were centrifuged, the medium was discarded and replaced with 100 μl assay buffer containing 0.1 M sodium acetate (pH = 5), 0.1% Triton X-100 and 5 mM *p*-nitrophenyl phosphate, pNPP (Sigma–Aldrich) and incubated for additional 2 h at 37 °C. The reaction was stopped with 10 μl/well of 1 M NaOH, and the absorbance values were measured at the wavelength of 405 nm using a microplate reader (Infinite M200Pro, Tecan, Austria).

2.3.2. Flow cytometric analysis of cancer cell death

Detection of cell death was carried out by staining with propidium iodide (PI). Cancer cells were seeded into 12-well plate and treated for 46 h with ligands **1**–**5** and complexes **1a**–**5a** at indicated concentrations. After treatment, cells were collected, centrifuged at 400 $\times$ *g* for 5 min and stained with PI for 15 min at room temperature in the dark. 15,000 events were analyzed for each sample by flow cytometer FACSVerse (Becton Dickinson), and results were processed by using FACSuite software (Becton Dickinson).

2.4. Cyclic voltammetry

The compounds were measured electrochemically by cyclic voltammetry. Complexes were dissolved in tetrabutylammonium tetrafluoroborate. All measurements were carried out at room temperature. Cyclic voltammograms were obtained on computer-controlled electrochemical system under argon atmosphere.

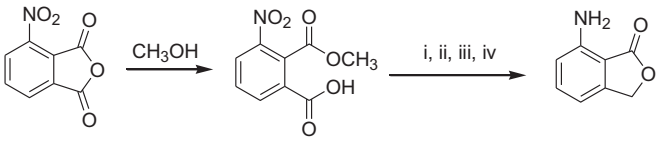

i: $ClCOOCH_2CH_3$, $N(CH_2CH_3)_3$; ii: $NaBH_4$; iii: HCl; iv: H_2, Pd/C, acetic acid

Scheme 1. Synthesis of 7-aminophtalide (**5**).

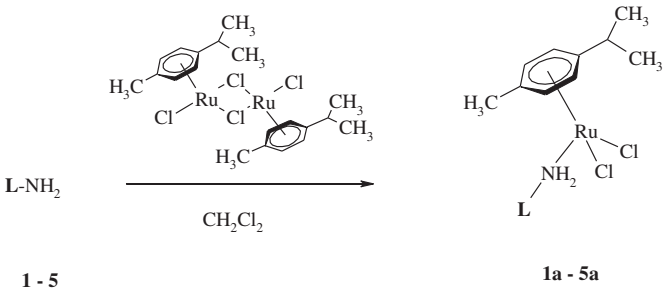

Scheme 2. Synthesis of complexes **1a**–**5a**.

Standard three electrodes were used: glassy carbon electrode (working), silver wire (pseudo reference) and platinum wire (auxiliary).

3. Results and discussion

3.1. Chemistry

To this work we have selected five ligands, the derivatives of flavone (**1**, **2**), chromone (**3**, **4**), and benzofuranone (**5**), see Fig. 1. In our previous papers we reported that ligand **3** form monodentate Zn(II) complex *via* oxygen atom in carbonyl group [17]. While ligand **4** can form monodentate Zn(II) complex *via* nitrogen atom in amino group in C-7 position [18], also bidentate coordination with $Cu(ClO_4)_2 \times 6H_2O$ *via* nitrogen and oxygen atoms has been reported [19].

Ligands **1**–**3** were commercially available. The ligand **4** was synthesized according to procedure described previously [17]. Based on the literature [20,21] we synthesized ligand 7-aminophtalide L(**5**) using as materials 3-nitrophthalic anhydride which is commercially available (Scheme 1).

All complexes **1a**–**5a** were prepared at room temperature in dichloromethane by mixing equimolar amounts of ruthenium *p*-cymene compound and corresponding or in solution of dichloromethane and isopropanol ligands L(**1**–**5**), respectively. All ligands behaves as a strong monodentate chelating agents forming new Ru(II) complexes through coordination of the amino nitrogen atom (Scheme 2).

3.2. IR spectra

The most important IR spectral data for ligands **1**–**5** and their complexes are listed in Table 1. The IR spectra of all compounds show characteristic stretching vibrations at ~3200–3400 cm^{-1} which correspond to the asymmetric and symmetric $\nu(NH_2)$. These bands are negatively shifted in complexes **1a**–**5a** in comparison to free ligands (by 114 and 47 cm^{-1} for compound **1a**, 115 and 80 cm^{-1} for compound **2a**, 229 and 221 cm^{-1} for compound **3a**, 8 and

Table 1
IR data (ν, cm^{-1}) for ligands **1**–**5** and complexes **1a**–**5a**.

Compound	$\nu(NH_2)$	ν(C=O)	ν_{aromat}
1	3342, 3238	1642	1581, 1565, 1487
1a	3228, 3191	1619	1600, 1579, 1470
2	3460, 3293	1630	1600, 1586, 1498
2a	3345, 3213	1647	1607, 1456
3	3431, 3322	1655	1584
3a	3202, 3101	1618	1593, 1542, 1493
4	3432, 3324	1648	1625, 1588, 1569
4a	3424, 3264	1640	1618, 1538, 1486
5	3480, 3376	1748	1642, 1600
5a	3264, 3181	1741	1608, 1567

60 cm^{-1} for compound **4a**, 216 and 195 cm^{-1} for compound **5a**). These bands shift to lower energy confirm that coordination of the amino group has occurred. The ν(C=O) bands are presented for each compounds at 1748–1618 cm^{-1}. Vibrations from aromatic carbons are assigned for bands in the 1642–1456 cm^{-1}.

3.3. ^1H NMR spectra

^1H NMR spectra data of complexes **1a**–**5a** were recorded in $CDCl_3$ and are presented in the experimental section. Position and intensity of the signals correspond to ligands used in synthesis. Methyl protons of the isopropyl group give signals at δ 1.28 ppm as doublets and methylene proton at δ 2.94 ppm as multiplet. The aromatic protons from *p*-cymene in the complexes are presented as four doublets at 4.98, 5.09, 5.38 and 5.45 ppm. This is probably due to the long range coupling of diastereotopic methyl protons of isopropyl group and aromatic protons of the *p*-cymene [22,23]. The methyl protons from ligands are displayed as singlets at 2.37 for complex **4a** and 2.10 ppm for complex **5a**.

3.4. UV–Vis spectra

The UV–Vis absorption spectra of complexes **1a**–**5a** were recorded in dichloromethane at room temperature. All the studied complexes showed intense absorption bands in the range 243–325 nm attributed to intraligand charge transfer. In addition, a low energy absorption bands were presented in the range 450–500 nm. On account of position and intensity these transitions are believed to be metal to ligand charge transfer (MLCT) [24].

3.5. MS–FAB

Mass spectrometry was carried out for all newly synthesized complexes. Parent peaks have been found in FAB–MS spectra at (*m*/*z*) 543 for complex **1a**, at (*m*/*z*) 544 for complex **2a** and at (*m*/*z*) 481 for complex **3a**. Ion peaks corresponding to the ligands have been observed at (*m*/*z*) 238 for compounds **1a**, **2a**, at (*m*/*z*) 176 for compounds **3a**, **4a** and at (*m*/*z*) 154 for compound **5a**. For more detailed mass spectra analysis see experimental section.

3.6. Crystal structure of complex *5a*

The structure of complex **5a** has been confirmed by X-ray analysis, for crystallographic data see Table 2. The molecular structure with atom numbering scheme is presented at Fig. 2, while selected geometric parameters are shown in Table 3. The complex has an essentially octahedral coordination geometry comprising the *p*-cymene ring carbons occupying one face of the octahedron leaving the other three sites to be coordinated by two chloride atoms and monodentate (7-amino-3*H*-benzofuran-1-one) ligand. The Ru–C(arene) distances vary considerably from 2.160(3) Å to 2.203(3) Å. The molecules of **5a** complex symmetrical by inversion form dimers *via* N1–H1B···Cl1 interaction (see Fig. 3). In the crystal lattice another weak C–H···Cl and C–H···O intermolecular

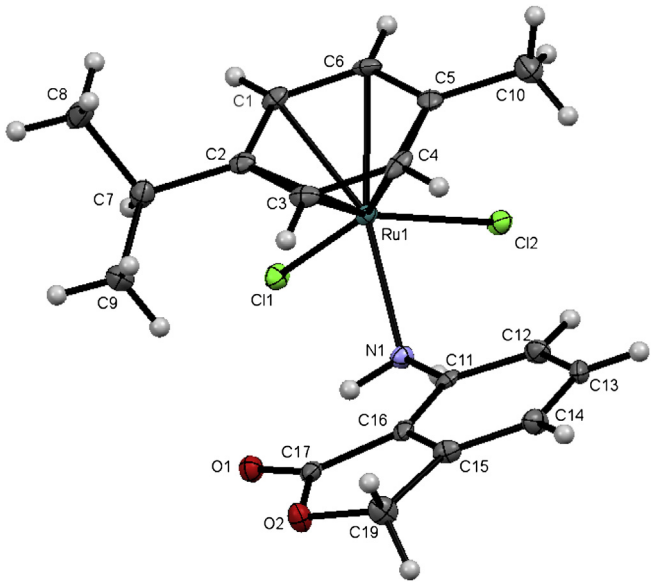

Fig. 2. An ORTEP view of complex **5a** with atom numbering scheme.

Table 2
Crystallographic data for compound **5a**.

	Complex **5a**
Molecular formula	$C_{18}H_{21}Cl_2NO_2Ru$
Molecular weight	455.33
Crystal description/size (mm)	Orange block/0.05 × 0.04 × 0.01
Crystal system	Monoclinic
Space group	$P2_1/n$
a [Å]	8.6021(3)
b [Å]	8.0777(2)
c [Å]	24.9788(9)
β [°]	90.160(3)
V [$Å^3$]	1735.65(2)
Z/d_x [g cm^{-3}]	4/1.742
F(000)	920
μ [cm^{-1}]	455.33
T [K]	100
maxθ [°]	25.35
No. of measured/unique reflections/R_{int}	11,469/3179/4.37%
$R_1/wR_2/S$ (goodness of fit)	0.0305/1.040
Difference peak/hole [e$Å^{-3}$]	0.523/−0.558

Table 3
Selected bond lengths (Å), angles (°) and hydrogen bond geometry (°, Å), symmetry codes (i): 2 − *x*, 1 − *y*, −*z*, (ii): 1 − *x*, 1 − *y*, −*z*, (iii): 5/2 − *x*, ½ + *y*, ½ − *z*.

Bond lengths (Å)			
Ru1 C1	2.165(4)	Ru1 C6	2.180(4)
Ru1 C2	2.197(3)	Ru1 N1	2.183(3)
Ru1 C3	2.160(3)	Ru1 Cl2	2.4063(8)
Ru1 C4	2.176(3)	Ru1 Cl1	2.4075(8)
Ru1 C5	2.203(3)		
Bond angles (°)			
C1 Ru1 N1	154.27(12)	C3 Ru1 Cl2	150.78(9)
C2 Ru1 N1	117.31(12)	C4 Ru1 Cl2	112.92(10)
C3 Ru1 N1	94.79(13)	C5 Ru1 Cl2	89.31(10)
C4 Ru1 N1	98.10(12)	C6 Ru1 Cl2	93.65(10)
C5 Ru1 N1	124.61(12)	C1 Ru1 N1	154.27(12)
C6 Ru1 N1	162.59(11)	C2 Ru1 N1	117.31(12)
C1 Ru1 Cl1	89.48(10)	C3 Ru1 N1	94.79(13)
C2 Ru1 Cl1	91.99(9)	C4 Ru1 N1	98.10(12)
C3 Ru1 Cl1	120.35(9)	C5 Ru1 N1	124.61(12)
C4 Ru1 Cl1	158.92(10)	C6 Ru1 N1	162.59(11)
C5 Ru1 Cl1	151.71(10)	Cl2 Ru1 Cl1.	88.09(3)
C6 Ru1 Cl1	113.89(9)	N1 Ru1 Cl1	82.78(7)
C1 Ru1 Cl2	122.93(10)	N1 Ru1 Cl2	81.45(8)
C2 Ru1 Cl2	161.10(10)		

Hydrogen bond geometry (°, Å)

	D–H	H···A	D···A	<D–H···A
N1–H1B···Cl1^{i}	0.90	2.48	3.290(3)	150
C1–H1···Cl2^{ii}	0.93	2.82	3.471(4)	128
C19–H19B···O1^{iii}	0.97	2.54	3.417(4)	151
C19–H19B···O2^{iii}	0.97	2.57	3.340(4)	137

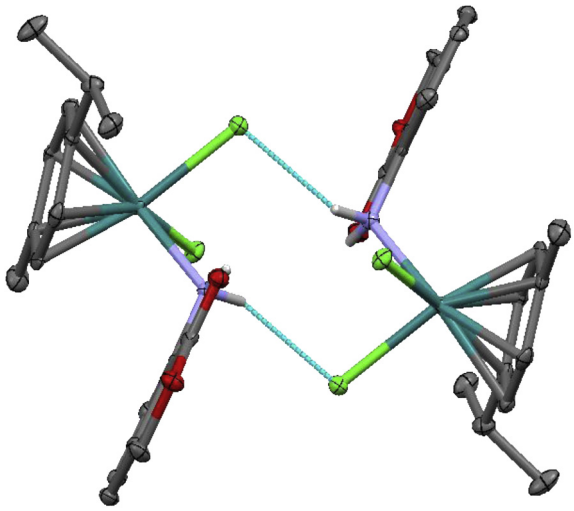

Fig. 3. Dimers of complex **5a** formed by N1–H1B···Cl1 interaction. Hydrogen atoms not involved in hydrogen bond are omitted for clarity, symmetry code (i): 2 − *x*, 1 − *y*, −*z*.

interactions which stabilized crystal packing are observed (Table 3). Additionally, the furan ring (O2/C17/C16/C15/C19) in the molecule at *x*, *y*, *z* is linked by π–π interactions with *p*-cymene ring (C1–C6) at *1* + *x*, *y*, *z*: the interplanar spacing is 3.406(2) Å, while the ring-centroid separation is 3.669(2) Å.

3.7. Cyclic voltammetry

The measurements were performed at glassy carbon electrode (working), silver wire (pseudo reference) and platinum wire (auxiliary) electrodes in tetrabutylammonium tetrafluoroborate. The cyclic voltammograms were obtained by scanning the potential between −2 and +2 V versus Ag/AgCl at a scan rate of 0.20 V/s. The potential data are given in Table 4.

On the forward scan for the negative to positive potential all complexes exhibited oxidation associated to the Ru(II)/Ru(III) process. On the return scan reduction process of the same redox couple was observed. Analysis of cathodic and anodic peaks established one metal centered voltammetric response with $E_{1/2}$ values in the range of −0.662 to −0.942 V assigned to (Ru(III)/Ru(II)) redox couple. The peak-to-peak separation value ΔE_p ranging from 536 to 970 mV suggest an irreversible one electron-transfer process. A representative voltammograms have been depicted in Figs. 4 and 5.

3.8. Biological activity

Ligands **1**–**5** and their complexes **1a**–**5a** were tested for their biological activity against human melanoma A375 cell line and leukemic K562 cell line. In addition, two melanoma cell lines, DMBC11 and DMBC12, derived from surgical specimens were

Table 4
Cyclic voltammetric data for complexes **1a**–**5a**.

Compound	E_{pc} (V)	E_{pa} (V)	$E_{1/2}$ (V)	ΔE_p (mV)
1a	−0.930	−0.394	−0.662	536
2a	−1.119	−0.313	−0.716	808
3a	−1.362	−0.523	−0.942	839
4a	−1.214	−0.250	−0.732	964
5a	−1.172	−0.202	−0.687	970

$\Delta E_p = E_{pa} - E_{pc}$, where E_{pa} and E_{pc} are anodic and cathodic potentials, respectively; $E_{1/2} = 0.5(E_{pa} + E_{pc})$.

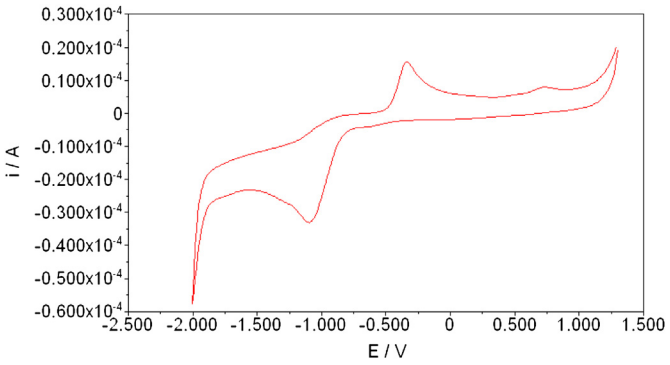

Fig. 4. Cyclic voltammogram of compound **3a**.

employed. Those melanoma cells were grown in anchorage-independent manner as spheroids [16]. Such as multicellular structures are considered to portray the original tumor more accurately than two-dimensional serum-driven monolayer cell cultures and they could be considered as a good *in vitro* model for anticancer drug screening. We have recently used this model to study the activities of different drugs and drug combinations [25–27]. In the current study cytostatic effects were assessed based on changes in the activity of acid phosphatase (APA assay). The results are shown in Fig. 6.

Changes in viability were measured by flow cytometry after labeling cells with propidium iodide. Cells that remained PI-negative are considered as viable. Viability expressed as % of control is shown in Fig. 7.

In general, ligand **3** and its complex **3a** showed the highest activity against both melanoma and leukemic cell lines. These two compounds were much more effective against heterogenous melanoma cell lines DMBC11 and DMBC12 than against established A375 melanoma cell line. In case of A375 cells it was mainly the cytostatic not cytotoxic activity as cell membrane did not become permeable to propidium iodide. Similar effects were obtained for A375 cells treated with cisplatin indicating that the mode of action might be similar for cisplatin and arene ruthenium(II) complexes [28]. Compound **1** and its derivative **1a** represented moderate activity against melanoma A375, DMBC11, DMBC12 cell lines. However, there is hardly any influence on leukemic K562 cell line. Other compounds turned to be less active in the performed tests. It was already shown that ruthenium complexes display promising anticancer activities [29,30]. Some of them, NAMI-A (ImH[*trans*-RuC14(DMSO)Im]) and KP1019 (indazolium *trans*-[tetrachloro bis(1*H*-indazole)ruthenate(III)]), have entered clinical trials. NAMI-A was shown to possess the ability to inhibit neoangiogenesis

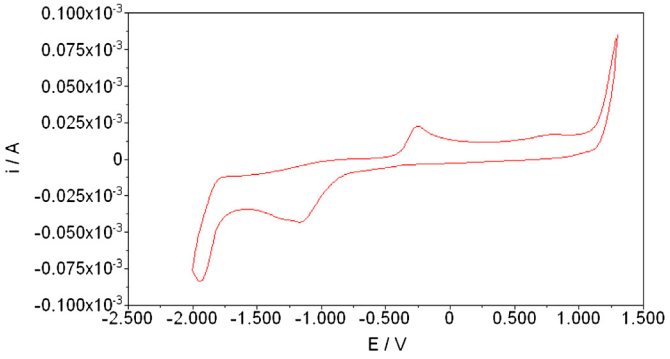

Fig. 5. Cyclic voltammogram of compound **4a**.

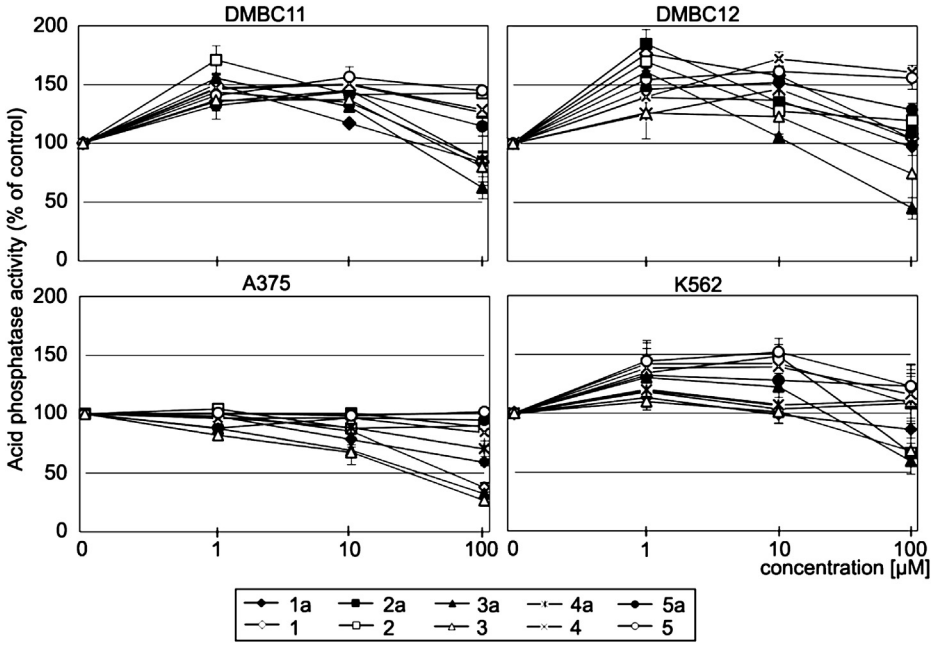

Fig. 6. The influence of ligands **1**–**5** and complexes **1a**–**5a** on viable cell numbers in melanoma and leukemic cell cultures. Melanoma cells A375 grown as the monolayer were more sensitive to tested compounds than heterogenous populations of anchorage-independent melanoma cells. Viability was assessed by acid phosphatase activity assay. Absorbance given by control cells was taken as 100%. Data represent the average ± SD.

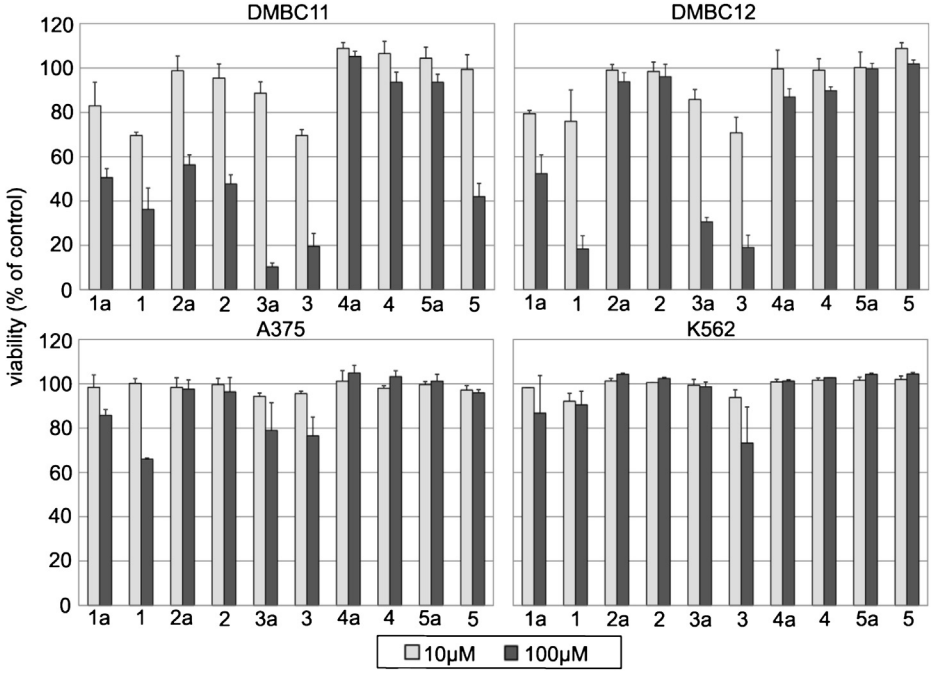

Fig. 7. Induction of cell death by ligands **1**–**5** and complexes **1a**–**5a** in melanoma and leukemic cell cultures. Cells were treated with tested compounds at concentrations of 10 and 100 μM for 44 h. Cells with PI-permeable membrane were assessed by flow cytometry. Percentages of viable cells (PI-negative) are shown as bars. The data are mean ± SD.

induced by vascular endothelial growth factor (VEGF) [31] and metastatic activity [32].

4. Conclusions

Arene ruthenium(II) complexes with flavone, chromone and benzofuranone derivatives as ligands were prepared. The complexes coordinated in a monodentate manner and were characterized by standard analytical techniques. The molecular structure of complex **5a** was determined by X-ray crystallography. The complex has an essentially octahedral coordination geometry comprising the *p*-cymene ring carbons occupying one face of the octahedron leaving the other three sites to be coordinated by two chloride atoms and monodentate (7-amino-3*H*-benzofuran-1-one) ligand. The molecules of the complex form dimers in the crystal lattice. Electron-transfer properties of all complexes have been

studied by cyclic voltammetry. The electrochemical analysis confirmed an irreversible one electron-transfer process occurring to all compounds which probably results in increased electrochemical stability of the compounds *in vivo*. In viability assays ligand **3** and its complex **3a** showed the highest activity against both melanoma and leukemic cell lines. Heterogenous patient-derived melanoma cell lines, DMBC11 and DMBC12, were more sensitive than established melanoma cell line, A375. Also compounds **1** and **1a** exerted some activity against melanoma cell lines A375, DMBC11 and DMBC12. In general, the biological study has revealed that leukemic cells were less susceptible to tested ligands **1**–**5** and complexes **1a**–**5a** than melanoma cells. This is in agreement with our previous results obtained for oximine rhenium(I) complexes for which higher anticancer activity was also induced against melanoma cells [33]. To our knowledge, the current report is the first study showing the biological activity of Ru(η^6-*p*-cymene) complexes with flavone and chromone against melanoma and leukemic cells. Further studies are necessary to resolve the mechanism(s) of the cellular responses evoked by these compounds and to assess their effectiveness in *in vivo* models.

Acknowledgments

Financial support from Medical University of Lodz (grant No. 503/3-066-02/503-01 to E. Budzisz and grant No. 503/1-156-01/503-01 to M. Czyz), grants No. 502-03/3-066-02/502-34-025 and 503/3-066-02/503-06-300 to A. Pastuszko and the DAAD fellowship No A/11/13479 are gratefully acknowledged. The authors wish to thank I. Dobinska for her support in biological experiments.

Appendix A. Supplementary material

CCDC 936546 contains the supplementary crystallographic data for this paper. These data can be obtained free of charge from The Cambridge Crystallographic Data Centre *via* www.ccdc.cam.ac.uk/data_request/cif.

References

[1] Y.K. Yan, M. Melchart, A. Habtemariam, P.J. Sadler, Chem. Commun. 38 (2005) 4764–4776.
[2] J. Kljun, A.K. Bytzek, W. Kandioller, K. Bartel, M.A. Jakupec, C.G. Hartinger, B.K. Keppler, I. Turel, Organometallics 30 (2011) 2506–2512.
[3] P. Heffeter, U. Jungwirth, M.A. Jakupec, C.G. Hartinger, M. Galanski, L. Elbing, M. Micksche, B.K. Keppler, W. Berger, Drug Resist. Upd. 11 (2008) 1–16.
[4] C.G. Hartinger, M.A. Jakupec, S. Zorbas-Seifried, M. Groessl, A. Egger, W. Berger, H. Zorbas, P.J. Dyson, B.K. Keppler, Chem. Biodiversity 5 (2008) 2140–2155.
[5] C.G. Hartinger, P.J. Dyson, J. Chem. Soc. Rev. 38 (2009) 391–401.
[6] G. Süss-Fink, Dalton Trans. 39 (2010) 1673–1688.
[7] M. Melchart, P.J. Sadler, in: G. Jouen (Ed.), Bioorganometallics, Biomolecular, Labeling, Medicine, Wiley-VCH, Verlag GmbH & Co., KGaA, Weiheim, 2006, p. 39.
[8] R.E. Murdoch, H. Chen, J. Cummings, N.D. Hughes, S. Parsons, A. Parkin, G. Boyd, D.J. Jodrell, P.J. Sadler, J. Med. Chem. 44 (2001) 3616–3621.
[9] L. Ronconi, P.J. Sadler, Coord. Chem. Rev. 251 (2007) 1633–1648.
[10] S. Martens, A. Mithöfer, Phytochemistry 66 (2005) 2399–2407.
[11] M. Di Braccio, G. Grossi, G. Roma, C. Marzano, F. Baccichetti, M. Simonato, F. Bordin, Farmaco 58 (2003) 1083–1097.
[12] E. Middleton Jr., C. Kandaswami, T.C. Theoharides, Pharmacol. Rev. 52 (2000) 673–751.
[13] M. Grazul, E. Budzisz, Coord. Chem. Rev. 253 (2009) 2588–2598.
[14] R.M.S. Pereira, N.E.D. Andrades, N. Paulino, A.C.H.F. Sawaya, M.N. Eberlin, M.C. Marcucci, G.M. Favero, E.M. Novak, S.P. Bydlowski, Molecules 12 (2007) 1352–1366.
[15] G.M. Sheldrick, Acta Cryst. A64 (2008) 112–122.
[16] M. Sztiller-Sikorska, K. Koprowska, J. Jakubowska, I. Zalesna, M. Stasiak, M. Duechler, M. Czyz, Melanoma Res. 22 (2012) 215–224.
[17] B. Kupcewicz, A. Kaczmarek-Kedziera, K. Lux, P. Mayer, E. Budzisz, Polyhedron 55 (2013) 259–269.
[18] B. Kupcewicz, M. Grazul, I.-P. Lorenz, P. Mayer, E. Budzisz, Polyhedron 30 (2011) 1177–1184.
[19] M. Grazul, A. Kufelnicki, M. Wozniczka, I.-P. Lorenz, P. Mayer, A. Jozwiak, M. Czyz, E. Budzisz, Polyhedron 31 (2012) 150–158.
[20] I.S. Ahuja, R. Singh, L. Sriramula, Trans. Med. Chem. I (1980) 373–376.
[21] P. Stanetty, I. Rodler, B. Krumpak, J. Prakt. Chem. 335 (1993) 17–22.
[22] K. Sarjit Singh, W. Kaminsky, Inorg. Chim. Acta 365 (2011) 487–491.
[23] A.K. Renfrew, A.E. Egger, R. Scopelliti, C.G. Hartinger, P.J. Dyson, C. R. Chim. 13 (2010) 1144–1150.
[24] A. Kumar Singh, P. Kumar, M. Yadav, D. Shankar Pandey, J. Organomet. Chem. 695 (2010) 567–573.
[25] M. Czyz, K. Koprowska, M. Sztiller-Sikorska, Cancer Biol. Ther. 14 (2013) 135–145.
[26] K. Koprowska, M.L. Hartman, M. Sztiller-Sikorska, M. Czyz, Anti-Cancer Drugs (2013), http://dx.doi.org/10.1097/CAD.0b013e3283635a04.
[27] M. Wozniak, A. Szulawska-Mroczek, M.L. Hartman, D. Nejc, M. Czyz, Anticancer Res. 33 (2013) 3205–3212.
[28] M. Czyz, K. Lesiak-Mieczkowska, K. Koprowska, A. Szulawska-Mroczek, M. Wozniak, Br. J. Pharmacol. 160 (2010) 1144–1157.
[29] O. Letzen, C. Moucher, A. Kirsch-De Mesmaker, John Wily & Sons, Ltd., West Sussex, 2005, pp. 359–378.
[30] T. Chen, Y. Liu, W.J. Zheng, J. Liu, Y.S. Wong, Inorg. Chem. 49 (2012) 6366–6368.
[31] F. Frausin, V. Scarcia, M. Cocchietto, A. Furlani, B. Serli, E. Alessio, G. Sava, J. Pharmacol. Exp. Ther. 313 (2005) 227–233.
[32] A. Bergamo, G. Sava, Dalton Trans. 40 (2011) 7817–7823.
[33] S. Wirth, A.U. Wallek, A. Zernickel, F. Feil, M. Sztiller-Sikorska, K. Lesiak, C. Bräuchle, I.-P. Lorenz, M. Czyz, J. Inorg. Biochem. 104 (2010) 774–789.